Eur. Phys. J. A **18**, 277–281 (2003)
DOI 10.1140/epja/i2002-10216-4

THE EUROPEAN PHYSICAL JOURNAL A

# Meson production at CELSIUS

T. Johansson[a]

Representing the CELSIUS/WASA Collaboration[b]
Department of Radiation Sciences, Uppsala University, Uppsala, Sweden

Received: 30 September 2002 /
Published online: 22 October 2003 – 

**Abstract.** The experimental programme of the CELSIUS/WASA Collaboration at the CELSIUS cooler/storage ring of the The Svedberg Laboratory, Uppsala, focuses on meson production and decay studies using light-ion collisions near threshold. The production of $\eta$-mesons has been studied in *pp* and *pd* collisions and $2\pi$ reactions have been studied in *pp* collisions, using the PROMICE/WASA detector. Both total and differential cross-sections have been investigated and some of the reaction channels have been measured for the first time in any detail. The data on $\eta$ production reveal effects which can be attributed to a strong and attractive $\eta$-$N$ interaction. Both the $\eta$ and two-pion production data contain new information on the importance of different nucleon resonances in these reactions. The PROMICE/WASA detector is now an integrated part of the recently commissioned WASA detector at CELSIUS, which has a nearly $4\pi$ acceptance for both charged particles and photons. This will provide significantly improved conditions for a new generation of experiments on meson production and decays.

**PACS.** 13.75.-n Hadron-induced low- and intermediate-energy reactions and scattering (energy $\leq$ 10 GeV) – 14.20.Gk Baryon resonances with $S = 0$ – 25.40.Ve Other reactions above meson production thresholds (energies $>$ 400 MeV)

## 1 Introduction

Cooler/storage rings, with their high-quality beams and thin windowless internal targets, offer an ideal environment for measurements of meson production in the threshold region. Such studies have therefore been a major topic of research at the CELSIUS, COSY and IUCF machines.

This paper reviews results from CELSIUS taken by the CELSIUS/WASA Collaboration on $\eta$-meson production in proton-proton and proton-deuteron collisions and $2\pi$ production in proton-proton collisions. The motivation for the study is twofold; to learn about a) the reaction mechanism, and b) the interaction between the final-state particles. The fact that only a few partial waves are important near threshold will facilitate any interpretation of the data. Furthermore, the relatively high and well-defined momentum transfers involved makes these processes good candidates to probe short-range physics. Kinematical considerations ensure that, close to threshold, the final-state particles are all emitted with low relative velocities, allowing the possibility of studying interactions between these particles.

The CELSIUS ring at the The Svedberg Laboratory, Uppsala, currently provides protons up to a maximum kinetic energy of 1.35 GeV. This makes $\eta$-mesons energetically accessible for experimental studies in free proton-proton collisions up to a centre-of-mass (CM) excess energy, $Q_{\rm cm}$ ($= \sqrt{s} - \sum m_{\rm final}$), of 37 MeV above the reaction threshold. This limitation has been circumvented by taking advantage of the Fermi motion of the struck nucleon in quasi-free reactions using deuterium as a target. A $Q_{\rm cm}$ of more than 100 MeV can be reached through this technique.

A complication when using internal targets at storage rings is that the beam pipe limits the access in the very forward direction. This drawback can be turned into an advantage by using a magnetic system that bends the produced charged particles out of the beam trajectory for subsequent detection. Alternatively, for short-lived mesons, one may detect the decay products. Both techniques have been employed at CELSIUS. The experiments with the PROMICE/WASA (PW) set-up used an internal cluster jet target, giving a typical target density of $10^{14}$ atoms/cm$^2$. With a circulating beam of a few times $10^{10}$ protons, this provides luminosities of the order of $5 \times 10^{30}$ cm$^2$ s$^{-1}$. More details of the PW set-up can be found in ref. [1].

[a] e-mail: tord.johansson@tsl.uu.se
[b] www.tsl.uu.se/wasa

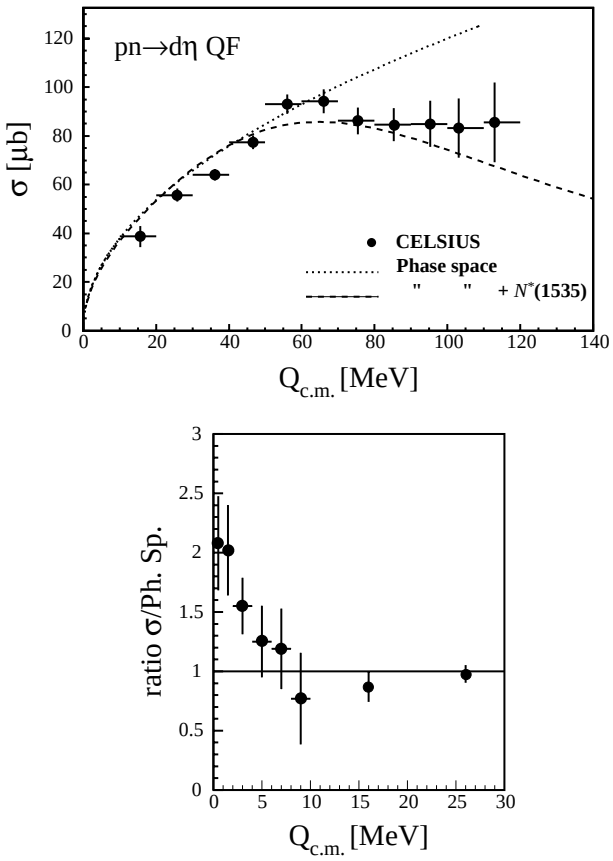


**Fig. 1.** Energy dependence for the quasifree $pn \to d\eta$ reaction. The upper figure shows data in the region $16 \leq Q_{\rm cm} \leq 113$ MeV [5]. Also shown is a two-body phase-space curve (dotted line) and a Breit-Wigner shape (dashed line) representing the $N^*(1535)$. The lower curve shows the ratio between the measured cross-section and the phase-space in the vicinity of the threshold [6].

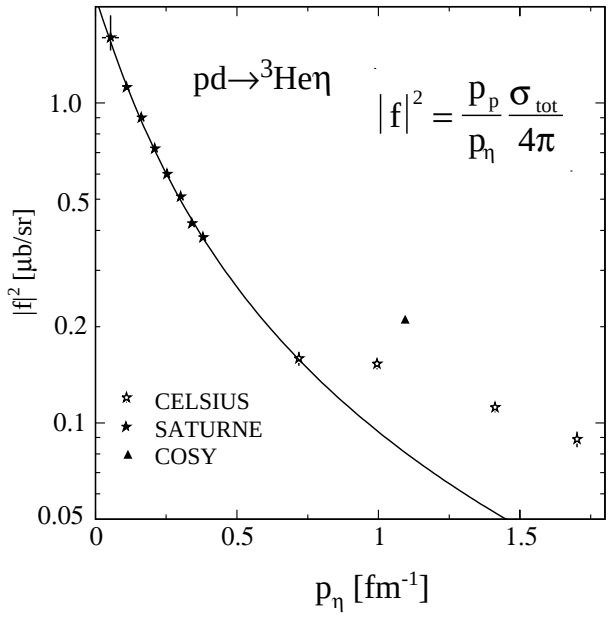


**Fig. 2.** Amplitude squared of the $pd \to {}^3{\rm He}\,\eta$ reaction, averaged over spin and angle, as a function of the CM $\eta$ momentum. Full and empty stars represent the result from SACLAY [10] and CELSIUS [12], respectively. The COSY point is denoted by a closed triangle. The solid line represents an $s$-wave optical model fit to Saclay ${}^3{\rm He}\,\eta$ and ${}^4{\rm He}\,\eta$ data [10,11] data.

## 2 Meson production experiments

### 2.1 $\eta$ production in pN collisions

Low-energy $\eta$ production is believed to be dominated by an isospin-$\frac{1}{2}$ $s$-wave resonance, the $N^*(1535)S_{11}$. This resonance has a large decay branching ratio (30%–55%) into the $N\eta$ channel and its width of $\approx 150$ MeV overlaps the $N\eta$ threshold. The presence of this resonance should influence the observables near threshold, where $s$-waves dominate, and also give rise to a strong and attractive $N\eta$ final-state interaction (FSI). It has even been suggested that this interaction might be strong enough for quasi-bound states to be formed already in the two-nucleon sector [2–4].

Effects relating to the $N^*(1535)$ have been observed in the $pn \to d\eta$ reaction. The two-body phase space gives a good description of the energy dependence of the cross-section up to a $Q_{\rm cm}$ of about 60 MeV, from where it starts to overpredict. This can be cured by including a Breit-Wigner function that describes the shape of the $N^*(1535)$-resonance [5], as shown in the upper part of fig. 1. This constitutes the first direct evidence for the importance of this resonance in nucleon-induced $\eta$ production. A relative enhancement of the cross-section with respect to phase space is observed very close to threshold [6]. This is shown in the lower part of fig. 1 and is an effect that would follow from an attractive $d$-$\eta$ FSI. Effects of a similar nature have also been observed for the $pp \to pp\eta$ reaction [7,8].

### 2.2 $\eta$ production in pd collisions

The renewed interest in $\eta$ production over the last 10 years started with measurements of the $pd \to {}^3{\rm He}\,\eta$ reaction at SATURNE [9,10]. These data are remarkable for both their magnitude and energy variation close to threshold. The amplitude squared falls over a factor of three in the first few MeV above threshold, as shown in fig. 2. This energy variation is certainly associated with an interaction between the $\eta$ and the ${}^3$He in the final state [11]. More recent data taken by the PW experiment at higher energies ($Q_{\rm cm} > 50$ MeV) [12] are also shown in fig. 2 together with a datum point from COSY [13].

The first CELSIUS point lies on a line which corresponds to an $s$-wave optical model fit of the earlier SATURNE data from ref. [10,11]. Data at higher energies lie above the curve. This is not surprising as higher partial waves become increasingly more important as the energy increases. This is also illustrated in fig. 3, which shows an increasing anisotropy of the angular distributions with energy.

The same data sample also contains information on the $pd \to pd\eta$ reaction. The first, very preliminary, results

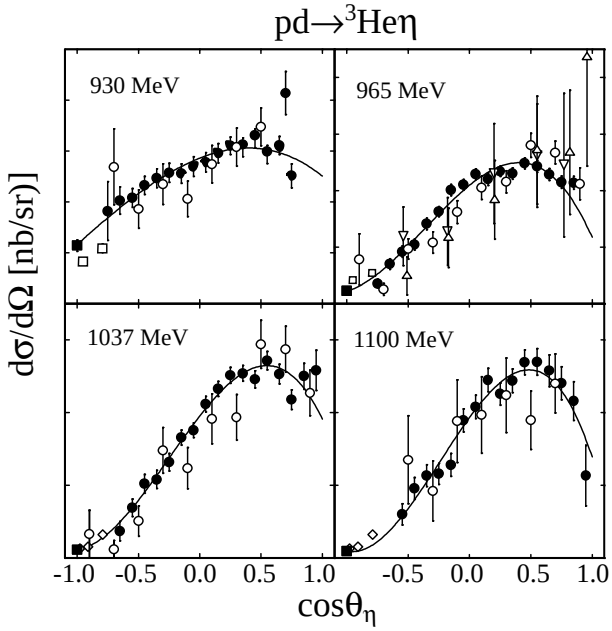


**Fig. 3.** Angular distributions for the $pd \rightarrow {}^3\mathrm{He}\,\eta$ reaction at four energies. The full and empty circles represent PW data [12] taken with only the $^3$He detected and with the $^3$He and two photons detected in coincidence, respectively. The full squares come from an interpolation in energy from SATURNE data [15]. The open squares and diamonds were taken from the same reference at 950 MeV and 1050 MeV, respectively. The triangles are COSY data [13] scaled by an empirical factor of 0.71 to agree with the trend of our data shown in fig. 2. The solid lines represent third-order polynomial fits to the data.

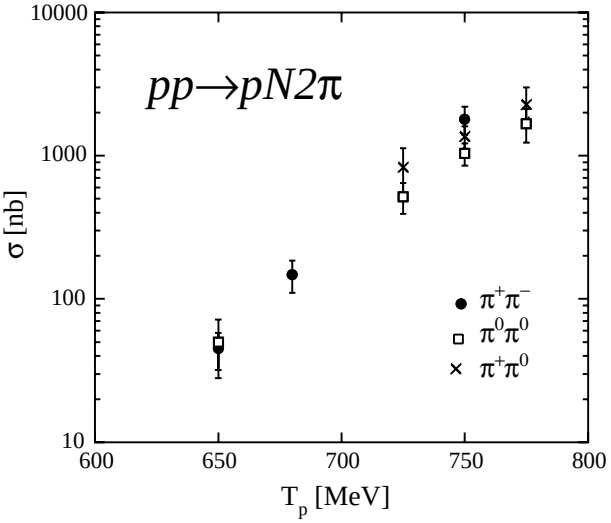


**Fig. 4.** Total cross-sections for the $pp \rightarrow pp\pi^+\pi^-$ (filled circles), $pp\pi^0\pi^0$ (open squares) and $pn\pi^0\pi^+$ (crosses) reactions between 650 and 775 MeV.

indicate much more isotropic angular distributions than for the $^3\mathrm{He}\,\eta$ final state [14]. The invariant mass spectra show a threshold $\eta\,d$ enhancement that is very similar to the one observed in the $pN$ interactions discussed in the previous section.

### 2.3 $2\pi$ production

Two-pion production in proton-proton collisions contains information about the nucleon-nucleon, pion-nucleon and pion-pion interactions. The production mechanism for these reactions is likely to be dominated by resonance production with the $N^*(1440)P_{11}$ and $\Delta(1232)P_{33}$ resonances being prime candidates. We have obtained data for the two-pion production from the $pp \rightarrow pp\pi^+\pi^-$, $pp\pi^0\pi^0$, $pn\pi^0\pi^+$ reactions at energies ranging from 650 to 775 MeV. This corresponds to excess energies from approximately 20 to 85 MeV, *i.e.* a region very close to threshold where no previous data are available. The PW results on the total cross-sections are shown in fig. 4.

We note that the magnitude for all three reactions is approximately the same. This information can be used within an isospin analysis to get a clue on the underlying reaction dynamics. The total $NN \rightarrow NN\pi\pi$ cross-section can be expressed in terms of isospin matrix elements $M_{T_\mathrm{i}T_{2\pi}T_\mathrm{f}}$, where $T_\mathrm{i}$ denotes the isospin of the initial nucleon pair, $T_\mathrm{f}$ is the isospin of the nucleons in the final state and $T_{2\pi}$ the isospin of the produced pion pair. Assuming that $\ell_{2\pi} = 0$, being close to threshold, it can be shown that the amplitude squared $|M_{121}|^2$ is about twice as large as $|M_{101}|^2$ [16]. Furthermore, the channel $N^*(1440) \rightarrow p + (2\pi)^{T=0}_{\ell=0}$ can only be involved in $|M_{101}|^2$, while $\Delta\Delta$ excitation is allowed in both $|M_{101}|^2$ and $|M_{121}|^2$. This could mean that the double-$\Delta$ excitation is the dominant reaction amplitude. However, the $N^*(1440)$ Roper resonance could still dominate the $pp \rightarrow pp\pi^+\pi^-$ cross-section due to the large isospin coupling factor for this matrix element [16]. The latter is confirmed from a study of the differential distributions from this reaction for the 750 MeV data [17]. Here it is shown that the differential distributions can be fully described by the $N^*(1440)$-resonance with decay branching ratios of $\approx 80\%$ for $N^* \rightarrow p + 2\pi$ decay and 20% for $N^* \rightarrow \Delta\pi$ decay. The contribution from the $\Delta\Delta$ channel turns out to be negligible at this energy. This is in agreement with the findings of Alvarez-Ruso *et al.* [18]. It should be noted, however, that they underpredict the magnitude of the $pp \rightarrow pn\pi^+\pi^0$ for which the $N^*(1440) \rightarrow N(\pi\pi)^{T=0}_{\ell=0}$ is forbidden by isospin conservation.

These findings show that the $pp \rightarrow pp\pi^+\pi^-$ reaction in the threshold region has the potential to give new information on the decay properties of the poorly known $N^*(1440)P_{11}$ Roper resonance. More details on this issue can be found in the contribution from H. Clement in these proceedings (see p. 171).

## 3 First results from the WASA detector

To investigate the different aspects of meson production in more detail, one needs high-quality data on the differential distributions from these reactions. The restricted

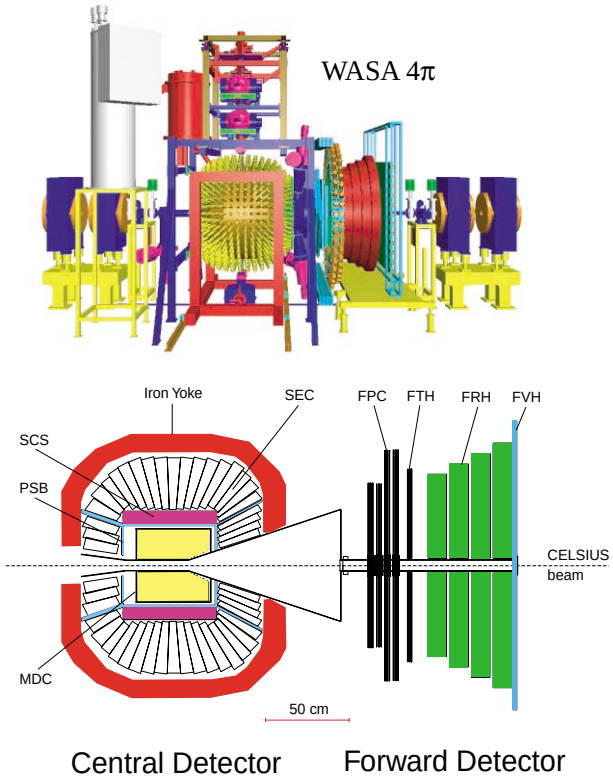


**Fig. 5.** The WASA $4\pi$ experimental set-up [19]. The upper figure shows a CAD view of the facility. The lower figure shows a cross-section of the detector. The forward detector is identical to the one used in the PW experiment [1].

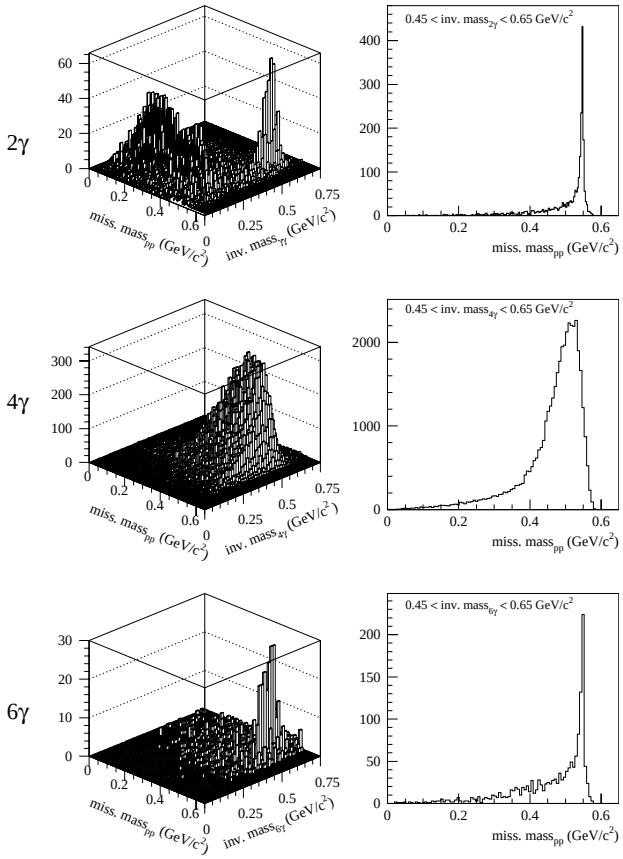


**Fig. 6.** Experimental data from the WASA detector at a proton kinetic energy of 1350 MeV with two protons identified in the forward detector and two, four and six $\gamma$'s measured in the central detector. The left column shows the invariant mass of the $\gamma$'s *versus* the two-proton missing mass. The right column shows the two-proton missing mass taken from a band around the $\eta$ mass in the invariant multiple $\gamma$ distributions.

acceptance of the PW experiment was a drawback in this respect. This limitation is overcome by the recently commissioned WASA $4\pi$ detector at CELSIUS [19], of which the PW set-up is a subset. The detector is designed for the measurements of rare $\eta$ and $\pi^0$ decays, where it should be capable of handling luminosities of about $10^{32}$ s$^{-1}$cm$^{-2}$ using frozen droplets (pellets) of hydrogen or deuterium as targets. It measures charged particles and photons over a solid angle close to $4\pi$ ($\approx 96\%$) with high accuracy both in energy and track coordinates. This is accomplished with a central detector (CD) whose outer part (SEC) is made from a large array of CsI(Na) crystals. The inner part is surrounded by a very thin-walled ($0.16X_0$) superconducting solenoid (SCS) and comprises a vertex detector (MDC) made from 16 layers of straw chambers organized in stereo-layers and a plastic scintillator barrel (PSB). The forward detector is the same as was used in the PW experiments. A CAD view of the WASA detector is shown in the upper part of fig. 5 and a cross-section of the detector is shown in the lower part.

An example of the present performance of the WASA detector is shown in fig. 6. The data were taken at a proton energy of 1350 MeV using a hydrogen pellet target. Two protons were identified in the forward detector with 2, 4 and 6 $\gamma$'s measured in the central detector. Prominent $\eta$ peaks can be seen in the $2\gamma$ and $6\gamma$ samples coming from the $\eta \to 2\gamma$ and the $\eta \to 3\pi^0$ decays. No $\eta$ signal is seen in the $4\gamma$ sample, as expected, since this decay is forbidden by $CP$ invariance. The continuum in the projection of the two-proton missing-mass plot comes mainly from the direct $pp \to \pi^0\pi^0\pi^0$ process and will lead to the first measurement of this cross-section in this energy region.

The power of the WASA detector to resolve the $pp \to pp\pi^0\pi^0$ reaction from the same data sample can be seen in fig. 7. Here the combinations of $2\gamma$ invariant masses that are closest to the $\pi^0$ masses are plotted. A clean $2\pi^0$ peak is then seen. No corrections have yet been made for acceptance and efficiencies.

## 4 Conclusions

$\eta$ production has been investigated in $pN$ and $pd$ interactions and $2\pi$ production has been studied in $pp$ interactions at the CELSIUS cooler/storage ring at the The Svedberg Laboratory. The results point to the importance of nucleon isobars in the production of these mesons. The $2\pi$ reaction is especially interesting in this respect and may

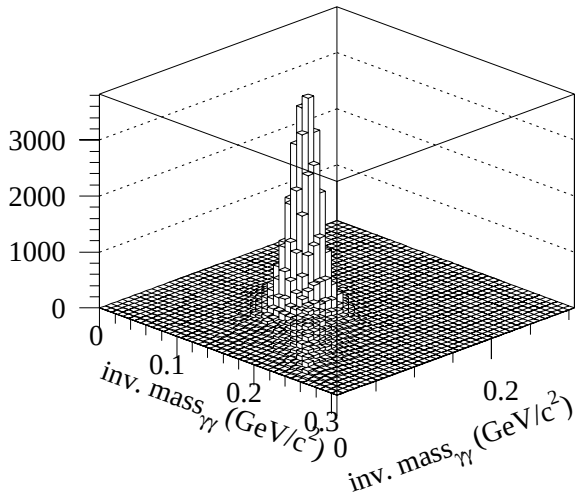


**Fig. 7.** Experimental data from the WASA detector at a proton kinetic energy of 1350 MeV with two protons identified in the forward detector and four $\gamma$'s measured in the central detector. The invariant-mass combination of the two $\gamma\gamma$ which best fit the $\pi^0$ assumption are plotted against each other.

prove to be an important tool to study the decay properties of the $N^*(1440)P_{11}$ Roper resonance. The newly commissioned WASA detector will be a powerful tool for continued studies of these reactions as well as for studies of other rare processes and meson decay properties.

## References


1. H. Calén *et al.*, Nucl. Instrum. Methods A **379**, 57 (1996).
2. T. Ueda, Phys. Rev. Lett. **66**, 297 (1991).
3. S.A. Rakityansky *et al.*, Phys. Rev. C **53**, R2043 (1996).
4. A.M. Green, J.A. Niskanen, S. Wycech, Phys. Rev. C **54**, 1970 (1996).
5. H. Calén *et al.*, Phys. Rev. Lett. **79**, 2642 (1997).
6. H. Calén *et al.*, Phys. Rev. Lett. **80**, 2069 (1998).
7. H. Calén *et al.*, Phys. Lett. B **366**, 39 (1996).
8. P. Moskal *et al.*, Phys. Lett. B **482**, 356 (2000).
9. J. Berger *et al.*, Phys. Lett. **61**, 919 (1988).
10. B. Mayer *et al.*, Phys. Rev. C **53**, 2068 (1996).
11. N. Willis *et al.*, Phys. Lett. B **406**, 143 (1997).
12. R. Bilger *et al.*, Phys. Rev. C **47**, 044608 (2002).
13. M. Betigeri *et al.*, Phys. Lett. B **472**, 267 (2000).
14. J. Złomańczuk, private communication.
15. P. Berthet *et al.*, Nucl. Phys. A **443**, 589 (1985).
16. J. Johanson *et al.*, Nucl. Phys. A **712**, 75 (2002).
17. W. Brodowsky *et al.*, Phys. Rev. Lett. **88**, 192301 (2002).
18. L. Alvarez-Ruso, E. Oset, E. Hernandez, Nucl. Phys. A **633**, 519 (1998).
19. J. Zabierowski *et al.*, Phys. Scr. T **99**, 159 (2002).